Construction and Building Materials 25 (2011) 3149–3157

Contents lists available at ScienceDirect

Construction and Building Materials

journal homepage: www.elsevier.com/locate/conbuildmat

Microstructure and mechanical properties of β-hemihydrate produced gypsum: An insight from its hydration process

Q.L. Yu *, H.J.H. Brouwers

Department of Architecture, Building and Planning, Eindhoven University of Technology, P.O. Box 513, 5600 MB Eindhoven, The Netherlands

ARTICLE INFO

Article history:
Received 10 December 2009
Received in revised form 19 November 2010
Accepted 7 December 2010
Available online 26 February 2011

Keywords:
β-hemihydrate
Hydration
Ultrasonic
Workability
Microstructure
Mechanical properties

ABSTRACT

This article addresses the microstructure and related mechanical properties of gypsum produced from β-hemihydrate using information of its hydration process, from fresh paste to hardened gypsum.

The water demand of the investigated β-hemihydrate was determined applying the spread flow test. The flowability was studied and the deformation coefficient of the β-hemihydrate was derived accordingly. The hydration process of the β-hemihydrate was investigated applying an ultrasonic wave method and the influence of the water content on hydration was analyzed.

The microstructure of the generated gypsum was studied by experiments and modeling. A model [1] was applied, which was successfully validated by the present experiments. Furthermore, the mechanical properties of the produced gypsum were investigated, and a numerical relation between water amount and strength was found.

1. Introduction

Gypsum ($CaSO_4{\cdot}2H_2O$, also known as dihydrate) plaster is one of the earliest building materials elaborated by mankind, and gypsum plasterboard is used widely as indoor building material because of its easy fabrication feature, environmental friendliness, fire resistance, aesthetics, low price, etc. The global production of gypsum in 2008 is over 250 million ton. Taking Europe as an example, there are 160 quarries for gypsum production and the number of employees is over 85,000 [2].

The $CaSO_4{\cdot}H_2O$ system is composed of five solid phases: dihydrate, hemihydrate ($CaSO_4{\cdot}0.5H_2O$), anhydrite I ($CaSO_4$), anhydrite II ($CaSO_4$), and anhydrite III ($CaSO_4$) [3]. Among them hemihydrate is usually used to produce gypsum plasterboard. Hemihydrate occurs in two forms, i.e. the α- and β-type, whereas β-hemihydrate is mainly applied since the hydration product of the α-hemihydrate is too brittle to be used as building material. The properties of gypsum are influenced by the hydration process and the properties of the hemihydrate.

The hydration of hemihydrate such as the hydration kinetics and setting has been studied intensively so far [4–11], but the emphasis was always laid on α-hemihydrate. Therefore topics such as the hydration induced properties, and especially the behavior of the β-hemihydrate upon hydration to produce gypsum (plasterboard) is still poorly understood. This article addresses the properties of gypsum (plasterboard) produced from a β-hemihydrate from its hydration process. The water demand of β-hemihydrate, as well as the flowability of the hydrating system was investigated by the common spread flow test. The hydration of β-hemihydrate was investigated applying an ultrasonic method and the influential factors on setting were studied. The microstructure as well as induced mechanical properties of the gypsum during hydration was investigated using experimental data and modeling.

2. Material and experimental

2.1. Material

The applied material, i.e. β-hemihydrate, in the present study was provided by Knauf Gips KG (Germany). The β-hemihydrate is produced from the flue gas desulfurization (FGD) gypsum. The β-hemihydrate was characterized in the present study in order to evaluate its physical properties such as: mineralogy, element, particle size distribution, specific surface area, and microstructure. X-ray diffraction (XRD) patterns were obtained using a Rigaku diffractometer operating at room temperature in order to confirm the mineralogy and crystallinity. The chemical analysis of the material was carried out using energy-dispersive X-ray spectroscopy (EDX). The particle size distribution (PSD) was measured with a Mastersizer 2000. The specific surface area was analyzed from both the measured PSD results and the BET method (TriStar 3000, Micromeritics). The microstructure of the hydrated system was measured with scanning electron microscope (SEM).

2.2. Water demand determination

Flowability is widely used to describe the properties of building materials like concrete or gypsum in fresh state and it is related to parameters such as fluidity, mobility, and compactability. To assure the hydrating system is fluid, a thin layer of adsorbed water molecules around the particles and an extra amount water to fill

* Corresponding author. Tel.: +31 (0) 40 247 2371: fax: +31 (0) 40 243 8595.
E-mail address: q.yu@bwk.tue.nl (Q.L. Yu).

0950-0618/$ - see front matter © 2010 Elsevier Ltd. All rights reserved.
doi:10.1016/j.conbuildmat.2010.12.005

Nomenclature

a	specific surface area, mass based (cm^2/g)
a_0	parameter
b_0	parameter
d	diameter (mm)
d_0	the base diameter of the Hägermann cone (100 mm) (mm)
E_h	the deformation coefficient
F_{rupt}	breaking load (N)
F_c	maximum load at fracture (N)
h	mass of the hemihydrate (g)
h_0	initial mass of the unreacted hemihydrate (g)
H	height of prism (cm)
K_{sp}	the solution product of gypsum
L_0	the distance between the supports of the bending machine (cm)
m	mass (g)
n	hydration degree
V	volume (cm^3)
W	width of prism (cm)
w	mass of the water (g)
w_0	initial mass of the water (g)

Greeks

α	activities of the free ions
β_h	the water/hemihydrate percentage (vol.%) for $\Gamma_h = 0$
Γ_h	the relative slump of the gypsum slurry
ρ	density (g/cm^3)
γ	the super saturation of gypsum
φ	volume fraction
δ	water layer thickness (cm)
ξ	shape factor
σ	strength (N/mm^2)
σ_0	strength at $\varphi_v = 0$ (N/mm^2)
ω	specific molar volume (cm^3/mol)
v	specific volume (cm^3/g)

Subscripts

Blaine	Blaine method
c	compressive strength
f	flexural strength
g	gypsum
h	hemihydrate
n	nonevaporable
s	shrinkage
sphere	sphere
w	capillary water
v	void fraction

the intergranular voids of the system is necessary [12]. Hence, the determination of water demand of fine powders is of vital importance. With the filled void fraction, the proportion of total specific surface area of the powders and the remaining water determines the workability [13].

Although many methods like angles flow box test, flow table test, or slump test can be used to determine the workability, the spread flow test was deployed in the present study because it is especially suitable to measure materials which have a collapsed slump. The spread flow tests were carried out first by filling the test sample into the Hägermann cone and then lifting it to allow a free flow of the sample to a dry, clean, horizontal and non sucking working surface (e.g. a glass plate was used here). The test was performed according to EN 13279-2 [14]. Ten mixes with different w_0/h_0 were measured in order to obtain a statistically reliable trend line for the regression analysis. A more detailed information about the test procedure can be found in [12].

2.3. Hydration process measurement

Eqs. (1) and (2) show the hydration of hemihydrate, which takes place quickly after mixing it with water via a through-solution route [15], firstly the hemihydrate dissolves (Eq. (1)) and then the generated dihydrate precipitates from the solution (Eq. (2)). Eq. (3) shows the integral hydration reaction as a combination of the foregoing two steps

$$CaSO_4 \cdot 0.5H_2O \rightarrow Ca^{2+} + SO_4^{2-} + 0.5H_2O \quad (1)$$

$$Ca^{2+} + SO_4^{2-} + 2H_2O \rightarrow CaSO_4 \cdot 2H_2O \quad (2)$$

$$CaSO_4 \cdot 0.5H_2O + 1.5H_2O \rightarrow CaSO_4 \cdot 2H_2O \quad (3)$$

The ultrasonic wave technology is widely used to detect the microstructure defects, variation and fracture of solids since the ultrasonic wave changes in different media [16]. Phani et al. [16] studied the strength and elastic modulus of gypsum using the ultrasonic technology. In the present research, the ultrasonic technology was deployed to measure the β-hemihydrate hydration process, since the microstructure of the hydrating system experiences a continuous change due to firstly the dissolution of the hemihydrate and then the generation and the precipitation of the dihydrate [7] during the whole process.

The hemihydrate hydration experiments with the ultrasonic method were performed at the University of Stuttgart, applying the FreshCon system as shown in Fig. 1 [17]. More detailed information about the FreshCon system and the measurement procedure was presented in [18].

2.4. Microstructure and mechanical properties measurement

Fig. 2 shows schematically the volume composition of the hydrating system. Before the hydration, the total volume is composed of only water and β-hemihydrate as shown in Fig. 2a. During the hydration reaction as shown in Eq. (3), part of the water and β-hemihydrate are consumed as reactants and gypsum is produced, so the total volume is composed of the chemical shrinkage due to the hydration reaction, the water that remains beyond the hydration reaction, the generated gypsum, and the remaining β-hemihydrate, shown in Fig. 2b.

The void fraction of the hydrating system here is defined as the fraction of void space in the hydrating system, where the void may contain air or water. Therefore the void fraction of the system upon the hydration reaction is described as the

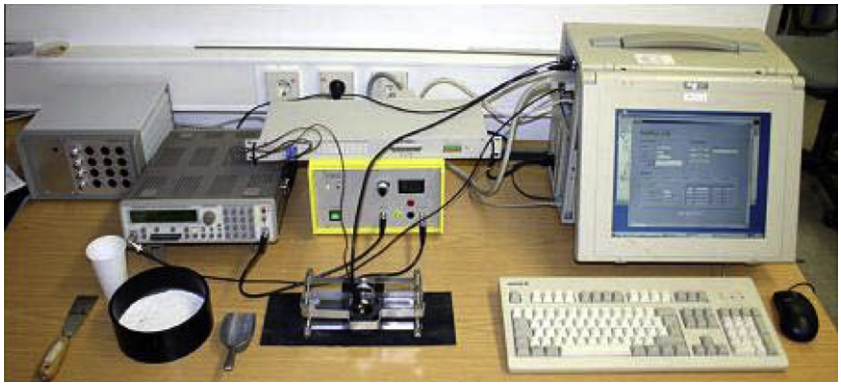

Fig. 1. The FreshCon system for ultrasonic velocity measurement [17].

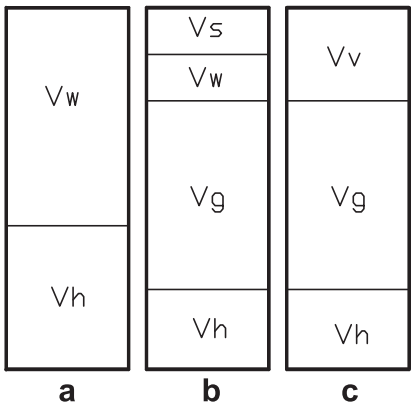

Fig. 2. Schematic diagram of the volume composition of the system (a: initial condition, $m = 0$ and b/c: upon hydration, $m > 0$).

addition of the volume caused by the reaction shrinkage and the remaining water as shown in Fig. 2c.

The microstructure of the hydrating system consequently influences the performance of the hydrated system such as the mechanical properties. The microstructure was investigated by both modeling and experiments, including SEM analysis and mechanical testing.

3. Results and discussion

3.1. Material characterization

Fig. 3a shows the XRD result of the used β-hemihydrate. The peak shows that the β-hemihydrate almost only consists of $CaSO_4{\cdot}0.5H_2O$. The chemical composition analysis measured by EDX method is listed in Table 1. It shows there are only very small impurities (Si, Mg and Al in total less than 3% by mass) in the sample, and also the amount of Ca and S is in line with the theoretical values, which also confirms the XRD result. The PSD of the β-hemihydrate is shown in Fig. 4, with the surface weighted mean (D [3,2]) of 6.07 μm. The specific surface area was calculated from the measured PSD results based on an assumption that all the particles are spheres [19], yielding 0.377 m^2/g (9877.4 cm^2/cm^3). A detailed calculation description can be found in [13,19]. The measured BET surface area of the β-hemihydrate is 7.50 m^2/g, and results show there are no micropores inside.

3.2. Water demand and flowability analysis

A concept of relative slump is used to analyze the water demand and workability in the present study. The relative slump is calculated from

$$\Gamma_h = (d/d_0)^2 - 1 \tag{4}$$

Here d is calculated from the average value of the two perpendicular diameters measured from the spread of the homogeneously prepared sample.

All the computed Γ_h based on Eq. (4) then are plotted versus the respective water/hemihydrate volume ratio (V_w/V_h) as shown in Fig. 5, the relation between V_w/V_h and w_0/h_0 is as follows:

$$\frac{V_w}{V_h} = \frac{w_0/\rho_w}{h_0/\rho_h} = \frac{w_0 \cdot v_w}{h_0 \cdot v_h} \tag{5}$$

A linear trend line is fitted through the plotted values, reading

$$\frac{V_w}{V_h} = E_h \Gamma_h + \beta_h \tag{6}$$

From Eq. (6), the water demand (β_h) of the β-hemihydrate, which represents that in this condition the slump flow equals to zero, is derived. This indicates the minimum water demand to assure a fluid gypsum plaster. In the present study, a β_h value of 1.436 was obtained, which is in line with [20]. This also confirms that the spread flow test is suitable for the determination of the water demand of the hemihydrate.

The deformation coefficient (E_h) is also derived from Eq. (6) (the slope of this function). This value indicates the sensitivity of the materials on the water demand for a specified workability, which means that the material with a lower deformation coefficient shows a bigger change in deformability to a certain change in water amount [13]. A deformation coefficient of 0.062 for cement (CEM III/B 42.5 N LH/HS) was given [21] which is bigger than that of β-hemihydrate (0.053) here. This indicates that water has a bigger influence on the workability of the hydrating system, which is probably due to the smaller surface area of the β-hemihydrate (9877 cm^2/cm^3) than that of the mentioned cement (15,300 cm^2/cm^3).

As discussed above, a thin layer of adsorbed water molecules around the particles is necessary to assure the fluidity of the hydrating system. Brouwers and Radix [21] reported that the thickness of this layer (δ) is related to the deformation coefficient and the surface area of the used material, which was later confirmed by [13], reading

$$E_h = \delta_{Blaine} \cdot a_{Blaine} \cdot \rho_h = \delta \cdot \xi \cdot a_{sphere} \cdot \rho_h \tag{7}$$

whereby ξ is the shape factor and a_{sphere} the surface computed using the PSD and assuming spheres. In the present study, using a a_{Blaine} value of 3025 cm^2/g [22] and a ρ_h value from Table 2, a δ_{Blaine} value of 66.8 nm is obtained, which is in line with [21] who reported a δ_{Blaine} value of 44.6 nm for CEM III/B 42.5 N LH/HS. Furthermore this is also confirmed by Marquardt [23] who reported a δ value of 45 nm with a different test, which was discussed in [12].

A linear relation was reported [13] between the specific surface area from Blaine method and computed specific surface area from PSD method, given by

$$\xi \cdot a_{sphere} = 1.7 \cdot a_{Blaine} \tag{8}$$

Substituting the surface areas yields $\xi = 1.36$.

3.3. Hydration process analysis

The measured ultrasonic velocity during the hydration with different w_0/h_0 is shown in Fig. 6 [17]. The velocity curve of the ultrasonic wave has the following characteristics. The first part is a dormant period, which is distinguished by a constant low velocity value; and is then followed with the second part in which the velocity increases rapidly until finally reaches a plateau, which is characterized also by a constant value.

The constant velocity value in the first period indicates the microstructure of the hydrating system remains stable or we can consider this period as the induction time of the β-hemihydrate in water. Eq. (9) gives the expression of the super saturation of the gypsum, where the K_{sp} equals 4.62 [4]. Nucleation and growth of the gypsum take place when $\gamma > 1$.

$$\gamma = \alpha(Ca^{2+})(SO_4^{2-})/K_{sp} \tag{9}$$

The ultrasonic velocity changes quickly after the induction time due to the change of the void fraction of the hydrating system and the physical properties of the materials in the system [24,25], which indicates the generation and precipitation of gypsum.

The measured values show that the ultrasonic velocity increases quickly in the precipitation period, but the increase rate gradually slows down until finally a plateau is reached. This can also be explained by Eq. (9) that the reduction of the free ions in

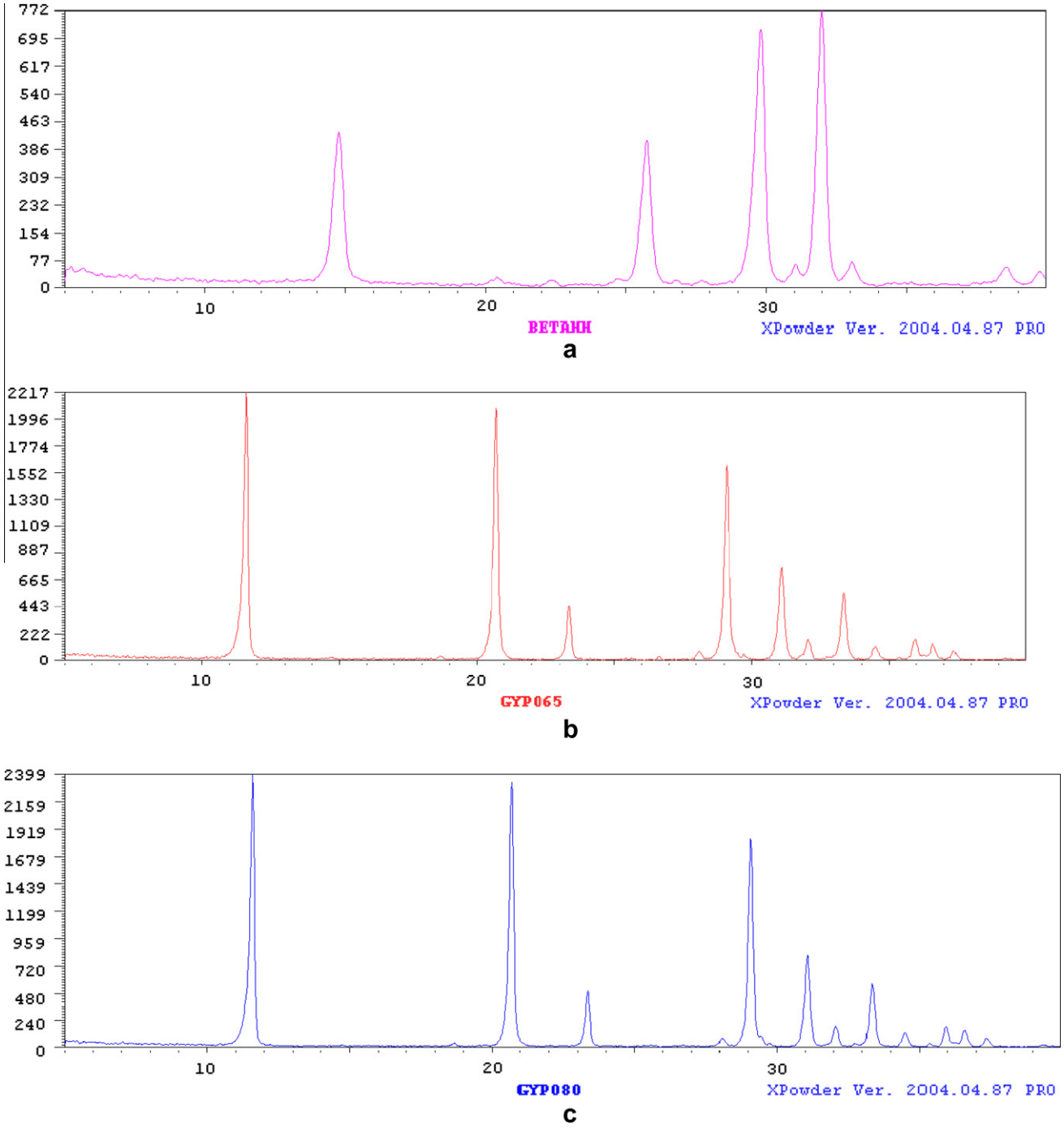

Fig. 3. The X-ray diffraction patterns (a: β-hemihydrate; b: gypsum produced with $w_0/h_0 = 0.65$; and c: gypsum produced with $w_0/h_0 = 0.80$).

Table 1
Chemical composition analyzed by EDX.

Element	wt.%	at.%	*K*-ratio
O	48.86	67.84	0.0714
Mg	0.87	0.80	0.0030
Al	0.80	0.66	0.0037
Si	1.32	1.05	0.0082
S	21.46	14.87	0.1758
Ca	26.68	14.79	0.2285
Total	100.00	100.00	

the solution due to the precipitation of the gypsum leads to the decrease of the hydration speed. The plateau of the ultrasonic velocity indicates the ending of the setting.

The measured results indicate that ultrasonic wave method is suitable for the hemihydrate hydration measurement. The measured initial setting time of about 4.5 min under the condition of the w_0/h_0 of 0.65 is in line with [20], in which the setting was measured with the knife methods [14]. The setting time measured using this method in this study is much shorter compared to the value from other method like electrical resistance method [7]. This probably can be explained by the difference between the microstructure of the used materials, which also indicates the used β-hemihydrate has an obvious influence on hydration.

The hydrating system with different w_0/h_0 shows different workability as analyzed above. This finding indicates the distance between the molecules of the hydrating system is different under

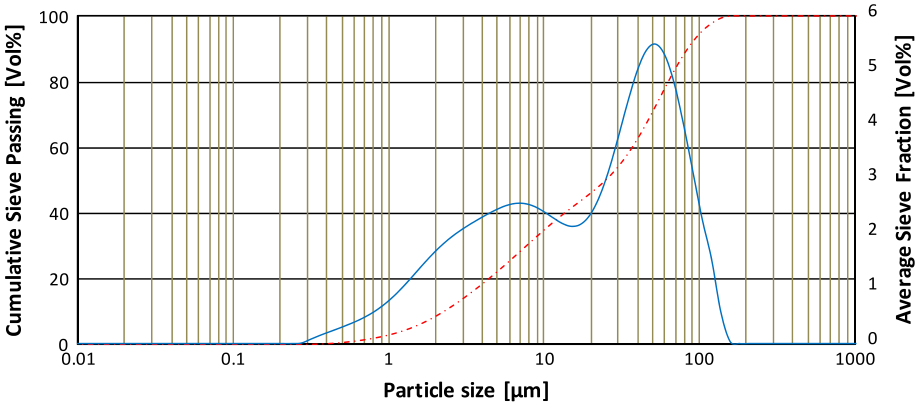

Fig. 4. The particle size distribution of the β-hemihydrate.

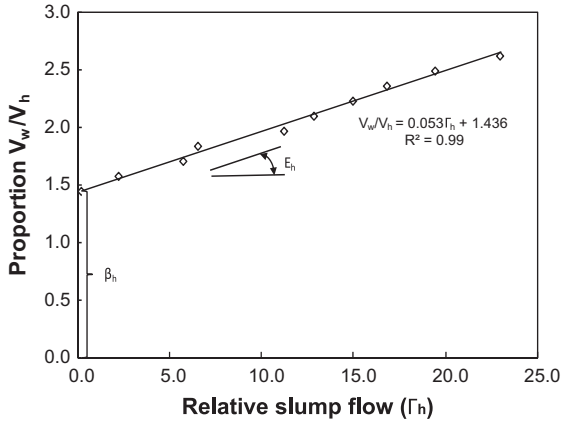

Fig. 5. Results of the spread flow test, plot of relative slump flow versus water/hemihydrate volume ratio.

different water content conditions. The distance between the molecules becomes larger when the water amount is higher which in turn should result in a longer reaction time. This is confirmed by the measured results with ultrasonic wave method shown in Fig. 6. The results show the induction time becomes longer with an increase of the water amount. The induction time is about 1.5 min with the w_0/h_0 of 0.65 while around 7 min when the w_0/h_0 increases to 1.25. The longer induction time with the higher w_0/h_0 as shown in Fig. 7 can also be explained by Eq. (9), the generated gypsum needs longer time to be super saturated. The relation between the water amount and induction time found in this study is shown in Fig. 7.

The influence of the water amount on the period of precipitation is reflected from the period duration and the velocity variation. With the w_0/h_0 of 0.65, the duration of this period is only around 7 min and the final velocity reaches to around 2500 m/s, while with the w_0/h_0 of 1.25, the duration of this period is about 18 min and the final velocity reaches about 2000 m/s. The duration of the precipitation period indicates evidently that the water amount influences greatly the hydration process of the hemihydrate. The result of the ending time of the hydration is shown in Fig. 7 too. Results indicate that water content at a lower w_0/h_0 has a dominant influence on the final setting of the hydrating system. This finding is confirmed by Schiller [26] who reported a similar trend of the relation between water ratio and setting time. But

Table 2
Parameters of the paste model [1].

Substance	M (g/mole)	ρ (g/cm^3)	ω (cm^3/mole)	v_h/v_w	w_n/h	v_n/v_w	$v_n w_n/v_w h$	v_s/v_h
Anhydrate	136.14	2.58	52.77	0.39	0.265	0.60	0.16	0.106
β-Hemihydrate	145.15	2.62	55.40	0.38	0.186	0.71	0.13	0.054
Dihydrate	172.18	2.32	74.22	0.43	–	–	–	–

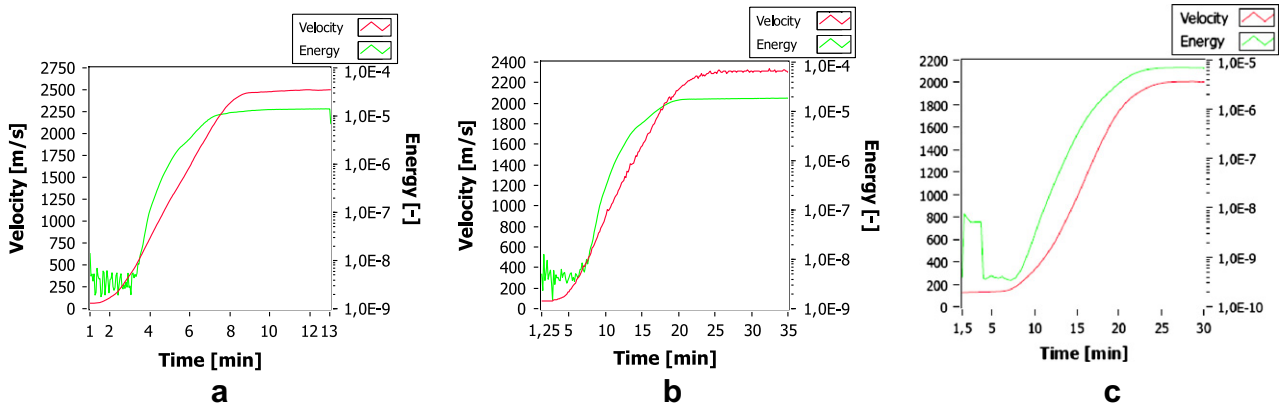

Fig. 6. Ultrasonic velocity during β-hemihydrate hydration (a: w_0/h_0: 0.65; b: w_0/h_0: 0.80; and c: w_0/h_0: 1.25) [17].

this finding is in contrast to Solberg and Hansen [9] who reported that hydration of the gypsum is almost independent of water amount within the w_0/h_0 range of 0.5–1.5.

Fig. 3b and c shows the XRD pattern of the hydrated gypsum with w_0/h_0 of 0.65 and 0.80, respectively. The results show obviously that the hydrated system only include $CaSO_4{\cdot}2H_2O$, which indicates that the β-hemihydrate is fully hydrated and the water content does not influence the final composition of the hydrated system. The difference between the final velocities indicates the final hydrated system has different microstructures due to the different initial water amount, which will be discussed in next section. This also can be explained from the so called void fraction of the system, which will be discussed in the next section as well.

3.4. Microstructure of the hydrating system

The chemical shrinkage of the hydrating system is computed from the difference between the reactant water and the chemical combined water following from Eq. (3). In this study a model proposed by Brouwers [1] is applied to describe the volume fraction of chemical shrinkage as follows:

$$\varphi_s = \frac{n\left(1-\frac{v_n}{v_w}\right)\frac{w_n}{h}}{\frac{v_h}{v_w}+\frac{w_0}{h_0}} \tag{10}$$

Table 2 lists the values of v_n/v_w, w_n/h, v_h/v_w for $CaSO_4$ systems [1].

Here the void fraction of the chemical shrinkage upon the hydration is defined as the proportion of the reaction shrinkage to the total volume that is constant during the whole reaction process, which is in line with Schiller [6] who also studied the void fraction of gypsum produced from α-hemihydrate based on the same assumption. The specific volume (cm^3/g) of the chemical combined water (v_n) used here is computed from the difference of the specific volume between the generated gypsum and the β-hemihydrate.

As discussed above, due to the requirement of the fluidity, an extra amount of water is needed. During the hydration reaction, the extra water works as transport liquid, and then it is evacuated during the curing period, which in turn leads to an open space of the generated gypsum. The void fraction caused by this unhydrated water reads

$$\varphi_w = \frac{\frac{w_0}{h_0}-n\left(\frac{w_n}{h}\right)}{\frac{v_h}{v_w}+\frac{w_0}{h_0}} \tag{11}$$

Therefore the void fraction during the hydration follows from the addition of the two parts, reading

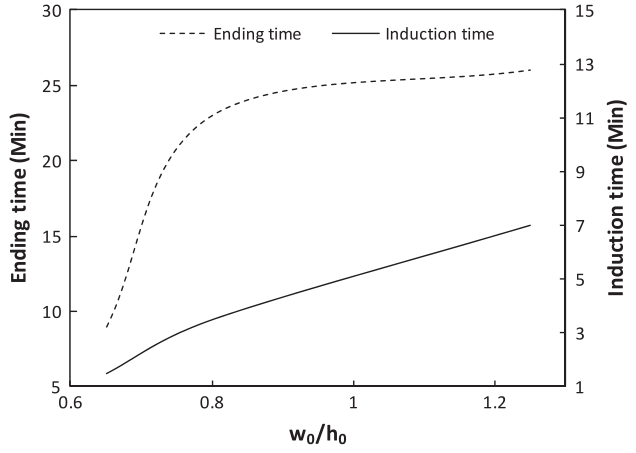

Fig. 7. Analysis of the hydration process.

$$\varphi_v = \varphi_w + \varphi_s = \frac{\frac{w_0}{h_0}-n\frac{v_n}{v_w}\frac{w_n}{h}}{\frac{v_h}{v_w}+\frac{w_0}{h_0}} \tag{12}$$

Substituting the values of the β-hemihydrate for the v_n/v_w, ω_n/h, v_h/v_w from Table 2, we obtain

$$\varphi_v = \varphi_w + \varphi_s = \frac{\frac{w_0}{h_0}-0.13n}{0.38+\frac{w_0}{h_0}} \tag{13}$$

It is evident from Eq. (13) that the void fraction is related to the water content and the hydration degree (n) of the hydrating system. Unlike cement, β-hemihydrate hydration occurs very quickly, for instance in the present study with the w_0/h_0 of 0.65 the full hydration ends within 10 min (see Fig. 7). Therefore the influence of water on void fraction in this study is mainly focused on the case that the hydration degree is unity, i.e. the system experiences the full hydration, yielding

$$\varphi_v = \frac{\frac{w_0}{h_0}-0.13}{0.38+\frac{w_0}{h_0}} \tag{14}$$

Schiller [6] proposed a void faction model for gypsum, which is in accordance with the model applied here (Eq. (13)), valid for the special case of full hydration and α-hemihydrate only.

The applied model is verified by experiments in the case of β-hemihydrate and full hydration. The measured void fraction of the gypsum is plotted versus w_0/h_0, together with the computed values from the applied model (Eq. (14)) shown as Fig. 8. The good agreement between predicted value and experimental data reveals the validity of the applied model.

The microstructure of the generated gypsum is shown in Fig. 9. The gypsum in Fig. 9a and b was prepared with a w_0/h_0 of 0.65 and 0.80, respectively. It is clear that the crystals in Fig. 9a are much tighter and homogeneous than that in Fig. 9b. This shows that the gypsum produced with a lower water content has a better bonding between the gypsum crystals which should lead better mechanical properties. Gypsum in Fig. 9a also shows a smaller void fraction compared to the gypsum in Fig. 9b, which is also in line with the applied model above.

3.5. Mechanical properties of gypsum

As typical for many building materials, gypsum behaves elastically under a load before reaching its elastic limit. However, it is obvious that the hardened gypsum is not a compact solid due to its high void fraction. Lewry and Williamson [27] reported that the gypsum strength develops during setting via a three-stage process: first a development of an interlocking matrix of dihydrate needles, then the relief of internal stress due to the build-up of pressure as needles, and final a strength increase during the removal of the excess water.

From the strength development process, one can see that the final strength of the gypsum is related to the formation of the produced gypsum crystals and the bond between them. From here we can assume that the water amount influences the strength of gypsum by influencing the void fraction since it influences the formation of the gypsum crystals and the bonds, which is confirmed by the SEM pictures as shown in Fig. 9a and b.

The strength tests were performed using a Zwick test device according to [14]. In this study the size of the samples was controlled strictly according to EN 13279-2 [14] to promise a representative value since Coquard et al. [28] reported that the sample size has an obvious influence on the strength of gypsum.

The flexural strength was measured with the three-point bending method, and the flexural strength is calculated from

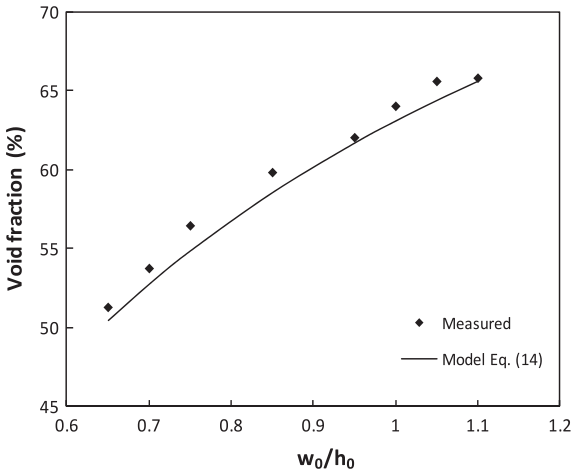

Fig. 8. The void faction versus the water-hemihydrate ratio (w_0/h_0).

$$\sigma_f = \frac{3F_{rupt}L_0}{2WH^2} \tag{15}$$

The compressive strength was determined by applying a load to the broken parts of the original specimen (40 mm × 40 mm × 160 mm) used for the flexural strength test, and the compressive strength is calculated from

$$\sigma_c = \frac{F_c}{1600\ \text{mm}^2} \tag{16}$$

The influence of the water content on strength of the gypsum was investigated and the measured flexural and compressive strength values are plotted versus void fraction as shown in Fig. 10. It is evident that the strength decreases with the increase of the void fraction, which can be explained by the bond between the crystals. When the water amount increases, the void fraction of the generated gypsum increases as analyzed above which in turn leads to a weaker bond between the gypsum crystals, which finally results in a decreased strength.

Several models [16,28] were proposed to describe the relation between the void fraction and the strength of gypsum, such as

$$\sigma = \sigma_0(1 - b_0\varphi_v) \tag{17}$$

$$\sigma = \sigma_0(1 - b_0\varphi_v)^{a_0} \tag{18}$$

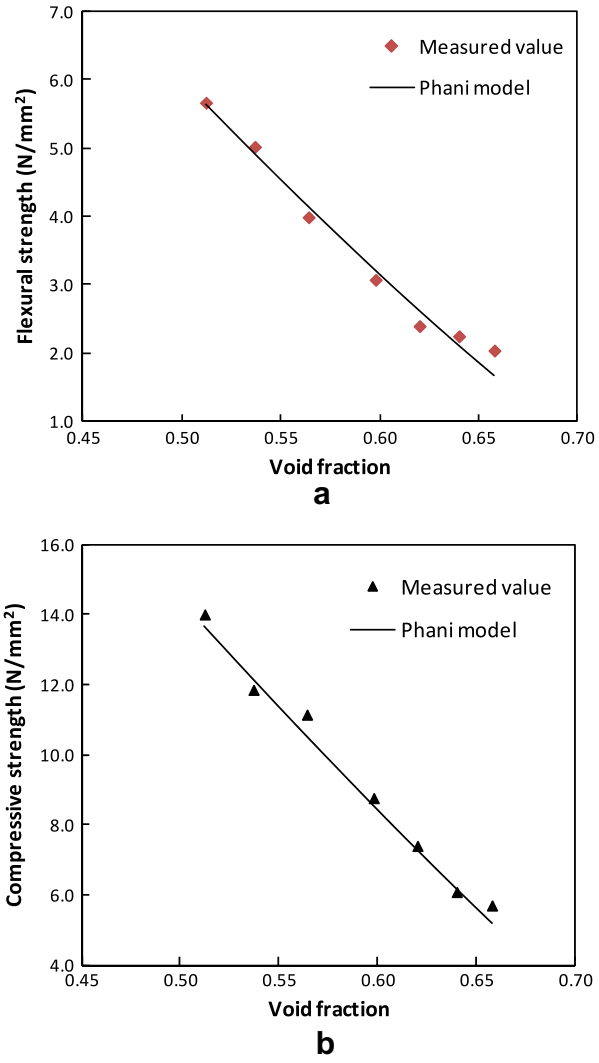

Fig. 10. The strength of the specimen versus the void fraction (a: flexural strength and b: compressive strength).

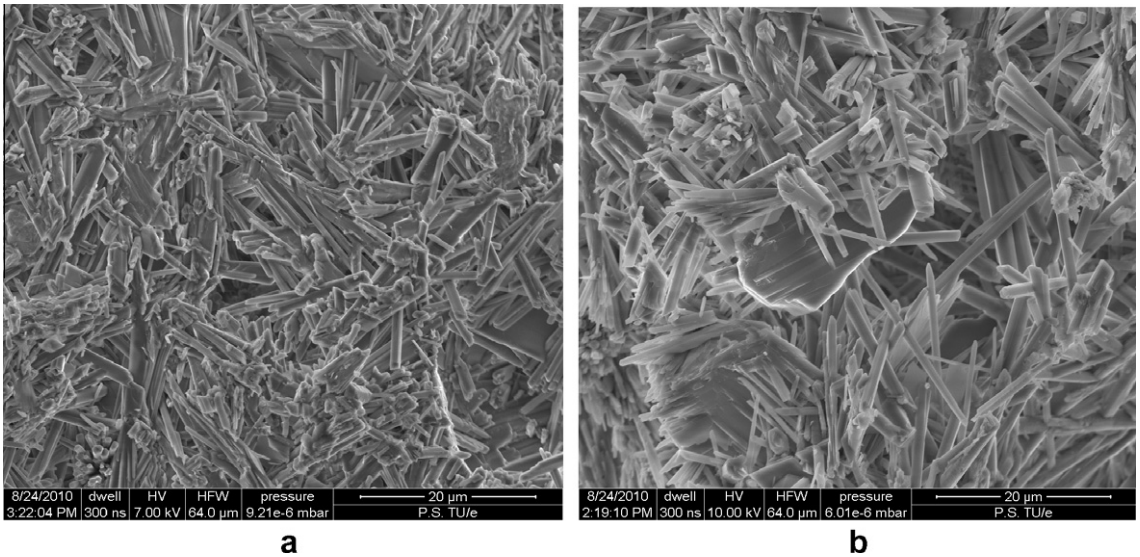

Fig. 9. The SEM picture of the gypsum (a: produced with $w_0/h_0 = 0.65$ and b: produced with $w_0/h_0 = 0.80$).

Table 3
Comparison of the four applied models.

Model	Flexural strength (σ_f, N/mm^2)				Compressive strength (σ_c, N/mm^2)			
	r^2	a_0	b_0	σ_0	r^2	a_0	b_0	σ_0
Lineal (Eq. (17))	0.97	–	1.38	18.94	0.98	–	1.33	43.33
Phani (Eq. (18))	0.98	1.20	1.35	23.10	1.00	1.16	1.30	48.70
Schiller (Eq. (19))	0.98	15.33	1.35	–	0.99	33.65	1.30	–
Exponential (Eq. (20))	0.99	–	7.49	269.60	0.98	–	6.33	369.31

$$\sigma = a_0 \ln\left(\frac{1}{b_0\varphi_v}\right) \tag{19}$$

$$\sigma = \sigma_0 \exp(-b_0\varphi_v) \tag{20}$$

In this study these models were applied and compared. The obtained coefficient of determination (r^2) and relevant parameters (a_0, b_0, and σ_0) are listed in Table 3. One point should be mentioned here is that both models from Schiller [6] and Phani et al. [16] were proposed based on α-hemihydrate produced gypsum. Actually the linear model (Eq. (17)) is one special case of the power model (Eq. (18)), i.e. when the exponent is unity. The power model gives best predictions in the present study. A critical void fraction value of 0.73–0.77 of the gypsum was obtained here ($1/b_0$ in Eqs. (17)–(19)). This value indicates that the produced gypsum will lose its strength at this void fraction, which is in line with Schiller [29] who reported a critical void fraction value of 0.79 for gypsum. This finding also indicates the strength is independent on the type of the used hemihydrate. An extreme strength (σ_0, flexural strength and compressive strength), i.e. the strength of gypsum at zero void fraction, is also derived from the models, as listed in Table 3. We can see that the Schiller model (Eq. (19)) has a limitation since it only can predict the critical void fraction other than the extreme strength, while the Exponential model (Eq. (20)) only gives an extreme strength other than the critical void fraction.

4. Conclusions

As an environmental friendly and sustainable building material, gypsum is widely used in the construction field. This study aims to contribute to a better understanding of the microstructure and related mechanical properties of gypsum produced from β-hemihydrate. The following conclusions can be drawn:

1. Water demand of β-hemihydrate was determined using spread flow test, and results show that spread flow test is a suitable test method. The workability was investigated and the influence of water content on the flowability was analyzed.
2. The deformation coefficient of the β-hemihydrate was derived, the thickness of a water layer around the particles to assure the fluidity of the hydrating system was discussed, and the shape factor of the investigated β-hemihydrate was derived.
3. The ultrasonic wave method is suitable for β-hemihydrate hydration measurement. A relation between the induction time and ending time of β-hemihydrate hydration and water content was found.
4. A model was applied to describe the microstructure of the hydrating system, which was validated by experiments. Subsequently a relation between water amount and the strength of generated gypsum was derived.

Acknowledgements

The authors wish to express their appreciations to Prof. Dr. H.U. Hummel and Mrs. K. Engelhardt from Knauf Gips KG (Germany) for materials supply; Prof. Dr. C.U. Grosse and Mr. F. Lehmann from University of Stuttgart (Germany) for executing the ultrasonic measurements. They furthermore express their gratitude to the European Commission (I-SSB Project, Proposal No.026661-2) for funding this research, as well as to the following sponsors: Bouwdienst Rijkswaterstaat, Graniet-Import Benelux, Kijlstra Betonmortel, Struyk Verwo, Insulinde, Enci, Provincie Overijssel, Rijkswaterstaat Directie Zeeland, A&G maasvlakte, BTE, Alvon Bouwsystemen, V.d. Bosch Beton, Selor, Twee "R" Recycling, GMB, Schenk Concrete Consultancy, De Mobiele Fabriek, Creative Match, Intron, Geochem Research, Icopal, and BN International (chronological order of joining). Thanks are also given to their colleagues: A.C.J. de Korte, M.M. Ballari, P. Spiesz, M.V.A. Marinescu, A. Lazaro Garcia, and G. Quercia Bianchi for their help.

References

[1] Brouwers HJH. A hydration model for Portland cement using the work of Powers and Brownyard, Skokie, Illinois, USA: Portland Cement Association; in press.
[2] Eurogypsum, 2010. <http://www.eurogypsum.org/industry_01.html>.
[3] Wirsching F. Calcium sulfate. Weinheim: Wiley-VCH Verlag GmbH & Co. KGaA; 2005.
[4] Amathieu L, Boistelle R. Crystallization kinetics of gypsum from dense suspension of hemihydrate water. J Cryst Growth 1988;88:183–92.
[5] Ridge MJ, Surkevicius H. Hydration of calcium sulphate hemihydrate I. Kinetics of the reaction. J Appl Chem 1962;12:246–52.
[6] Schiller KK. Porosity and strength of brittle solids (with particular reference to gypsum). In: Mechanical properties of non-brittle materials. London (UK): Butterworths Scientific Publications; 1958. p. 35–49.
[7] Lewry AJ, Williamson J. The Setting of gypsum plaster. Part 1. The hydration of calcium sulphate hemihydrate. J Mater Sci 1994;29:5279–84.
[8] Lancia A, Musmarra D, Prisciandaro M. Measuring induction period for calcium sulphate dihydrate precipitation. AICHE J 1999;45(2):390–7.
[9] Solberg C, Hansen S. Dissolution of $CaSO_4{\cdot}1/2H_2O$ and precipitation of $CaSO_4{\cdot}2H_2O$: A kinetic study by synchrotron X-ray powder diffraction. Cem Concr Res 2001;31(4):641–6.
[10] Gmouh A, Eve S, Samdi A, Moussa R, Tricha L, Aazzab B, et al. Development and validation of a dimensional variation measurement set-application to the plaster setting. Mater Sci Eng A – Struct 2004;372:123–7.
[11] Sattler H, Bruckner HP. Changes in volume and density during the hydration of gypsum binders as a function of the quantity of water available. ZKG Int 2001;9:522–9.
[12] Hunger M, Brouwers HJH. Flow analysis of water–powder mixtures: application to specific surface area and shape factor. Cem Concr Compos 2009;31:39–59.
[13] Hunger M. An integral design concept for ecological self-compacting concrete. PhD thesis. Eindhoven, The Netherlands: Eindhoven University of Technology; 2010.
[14] EN 13279-2, European Standard. Gypsum binders and gypsum plasters. CEN; 2004
[15] de Korte ACJ, Brouwers HJH. Hydration of modeling of calcium sulphates. In: Al-Mattarneh H, Mustapha KN, Nuruddin MP, editors. Proceedings of international conference on construction and building technology. Malaysia: Kuala Lumpur; 2008. p. 433–44.
[16] Phani KK, Niyogi SK, Maitra AK, Roychaudhury M. Strength and elastic modulus of a porous brittle solid: an acousto-ultrasonic study. J Mater Sci 1986;21:4335–41.
[17] Grosse CU, Lehmann F. Ultrasound measurements of hydrating of hemihydrates. Universitat Stuttgart; personal communication, 2008.
[18] Reinhardt HW, Grosse CU. Continuous monitoring of setting and hardening of mortar and concrete. Constr Build Mater 2004;18(3):145–54.
[19] Mastersizer 2000 user manual, Malvern Instruments Ltd; 2007. p. 73–4.
[20] Yu QL, Brouwers HJH, de Korte ACJ. Gypsum hydration: a theoretical and experimental study. In: Fischer HB, editor. Proceedings of 17th international conference in building materials (Internationale Baustofftagung). Germany: Weimar; 2009. p. 1-0783–8.

[21] Brouwers HJH, Radix HJ. Self-compacting concrete: theoretical and experimental study. Cem Concr Res 2005;35:2116–36.
[22] Engelhardt K. Pers Commun 2009.
[23] Marquardt I. Determination of the composition of self-compacting concretes on the basis of the water requirements of the constituent materials – presentation of a new mix concept. Betonwerk + Fertigteil – technik – BFT 2002;11:22–30.
[24] Harker AH, Temple JAG. Velocity and attenuation of ultrasound in suspensions of particles in fluids. J Phys D Appl Phys 1988;21(11):1576–88.
[25] Robeyst N, Gruyaert E, Grosse CU, De Belie N. Monitoring the setting of concrete containing blast-furnace slag by measuring the ultrasonic *p*-wave velocity. Cem Concr Res 2008;38:1169–76.
[26] Schiller KK. The course of hydration: its practical importance and theoretical interpretation. J Appl Chem Biotechnol 1974;24:379–85.
[27] Lewry AJ, Williamson J. The Setting of gypsum plaster part 2 the development of microstructure and strength. J Mater Sci 1994;29:5524–8.
[28] Coquard P, Boistelle R, Amathieu L, Barriac P. Hardness, elasticity modulus and flexion strength of dry set plaster. J Mater Sci 1994;29:4611–7.
[29] Schiller KK. Strength of highly porous brittle materials. Nature 1957;180:862–3.